Hindawi
Mathematical Problems in Engineering
Volume 2018, Article ID 4239658, 7 pages
https://doi.org/10.1155/2018/4239658

Research Article

Analytical Formulation for Temperature Evolution in Flat Wheel-Rail Sliding Surfaces

Hossein Alizadeh Otorabad,[1,2] **Parisa Hosseini Tehrani**,[1] **Davood Younesian**,[1] **Jilt Sietsma**,[2,3] **and Roumen Petrov**[2,3]

[1]*Center of Excellence in Railway Transportation, School of Railway Engineering, Iran University of Science and Technology, Tehran 16846-13114, Iran*
[2]*Department of Materials Science and Engineering, Delft University of Technology, Mekelweg 2, 2628 CD Delft, Netherlands*
[3]*Department of Electrical Energy, Metals, Mechanical Constructions and Systems, Ghent University, Technologiepark 903, 9052 Ghent, Belgium*

Correspondence should be addressed to Hossein Alizadeh Otorabad; h.alizadehotorabad@tudelft.nl

Received 21 August 2018; Revised 21 October 2018; Accepted 30 October 2018; Published 12 November 2018

Academic Editor: Ricardo Branco

Studying the temperature evolution of the thermally affected zone (TAZ) of sliding surfaces is crucial because of its influence on microstructural evolution, wear, and fatigue. Due to the complexity of thermal analysis of sliding bodies, relationships that predict their surface temperature evolution are very helpful because they can be used as time-dependent boundary conditions; this makes the thermal analysis of sliding bodies independent. In this paper, by assuming thermal contact conductance (TCC) at the sliding common surface, the differential equation governing the thermal analysis of the wheel-rail sliding is solved throughout a wheel flat. The temperature evolution of wheel and rail surfaces and the heat partitioning factor are among the main results. Finally, the equations obtained for wheel and rail surface temperatures are applied to a freight wagon and a passenger car as two real cases. The results are discussed and compared to existing data in the literature and a solid agreement is achieved.

1. Introduction

Temperature evolution of the thermally affected zone (TAZ) around contact surfaces of sliding bodies is crucial due to its influence on wear [1–3], fatigue [4], thermal softening [5], friction properties [6], microstructure evolution and residual stress [7], and so on. During pure sliding of a wheel onto rail, the temperature of contact surfaces increases. At the beginning of sliding, the contact patch is small and the heat flux is high. The temperature of contact surfaces increases rapidly. Because of decaying the mechanical properties of steel, a wheel flat is created and grows on the wheel tread due to wear. Rate of enlarging the contact surface is initially very high and the wheel flat reaches its final size very fast. During this process, the heat flux decreases and the wheel surface temperature reaches a stable value. Ahlström and Karlsson [8] found that the average steady-state temperature of wheel flats is 900±100°C.

Blok [9], Carslaw and Jaeger [10], and Archard [11, 12] are among the pioneer researchers who presented analytical expressions to estimate the temperature rise on sliding surfaces. These works have been fundamental to many researchers in this field till now. A survey on sliding surface temperature studies in chronological order has been presented in [13].

Ling and Ng [14] used Green's function method to express the temperature rise in the slider and rider. Gonzalez-Santander et al. [15] presented an analytical solution for the temperature evolution of the grinding wheel and the workpiece in dry grinding. Gonzalez-Santander and Martin [16] investigated the heat transfer in surface grinding. They found a rapid theoretical method for computation of the maximum temperature. Barber [17] derived a solution for the heat conduction in a single asperity interaction of sliding bodies of comparable hardness. Ling and Pu [18] used a stochastic model to show fluctuations of surface temperature.

Ahlström and Karlsson [8] investigated the microstructural evolution of TAZ around wheel flats in a railway wheel using a prescribed time-dependent temperature:

$$v = v_{ss}\left(1 - e^{\lambda t}\right), \quad (-\infty < \lambda < -2) \tag{1}$$

where v is temperature, v_{ss} is steady-state temperature, and λ is a rate parameter. They used this equation as a boundary condition in thermal analysis of wheel flats. They mentioned that, in sliding friction, λ is not easily determined because of lack of recordings of surface temperature as a function of sliding time. Choosing a proper equation as a model for predicting surface temperature evolution is valuable because it leads to accurate results.

In this study, we are dealing with equations thst are more accurate than existing models such as (1). The temperature evolution of wheel and rail during pure sliding using analytical method is investigated. One-dimensional heat analysis in semi-infinite solids is assumed at each point on the contact surface. Sliding occurs at a wheel flat and rail common surface and the contact pressure distribution is even during sliding. The reason is that the higher the contact pressure, the greater the wear during sliding. Wear is not considered here and contact patch is kept at the final size of the wheel flat. During full-braking when the wheels get locked, in a very short period of time at the beginning of sliding, the temperature is high enough to melt the surface layers or tremendously decay mechanical properties due to remarkably high heat flux. These layers get removed very rapidly during the skid and wheel flat is created. In our study, we solve the equations of the heat transfer right after formation of the wheel flat. Material properties are assumed to be constant with temperature. But the solution can be extended to the case in which the material thermal properties other than thermal diffusivity (κ) are temperature-dependent, as described in Theory. The rail temperature at the leading edge of the wheel flat is always at the rail's ambient temperature because fresh rail enters into contact surface at each moment during sliding. It is assumed that the temperature difference between wheel and rail is the same throughout contact surface. Finally, two real cases (a freight wagon and a passenger car) are investigated. The results are discussed and compared to existing data in the literature and a good agreement is achieved.

2. Theory

The differential equation governing the thermal analysis of the wheel-rail sliding at zero degree Celsius initial temperature, assuming a constant diffusivity (k_i) and no heat generation, is

$$\frac{\partial v_i\left(y_i,t\right)}{\partial t} - \kappa_i \frac{\partial^2 v_i\left(y_i,t\right)}{\partial y_i^2} = 0, \quad (i = w, r)$$
$$v_i\left(y_i, t = 0\right) = 0. \tag{2}$$

v_i is the temperature of ith body and i is wheel (w) or rail (r). t is time, k_i is the diffusivity of ith body and is defined as $\kappa_i = K_i/\rho_i c_i$, where K_i, ρ_i, and c_i are the thermal conductivity, mass density, and heat capacity of the ith body, respectively. Although in this study K_i, ρ_i, and c_i are assumed to be constant, if they are temperature-dependent, (2) holds its form with introducing a new variable θ_i as follows [10]:

$$\frac{\partial \theta_i\left(y_i,t\right)}{\partial t} - \kappa_i \frac{\partial^2 \theta_i\left(y_i,t\right)}{\partial y_i^2} = 0,$$
$$(i = w, r), \quad \theta_i = \frac{1}{K_0}\int_o^v K_i dv, \tag{3}$$
$$\theta_i\left(y_i, t = 0\right) = 0.$$

K_0 is the value of K when $v = 0$. In (3), κ_i is a function of θ_i and the differential equation is nonlinear. In reality, the dependency of κ_i on temperature is less important than that of K_i [10]. Therefore, it is a reasonable approximation to take κ_i as a constant parameter.

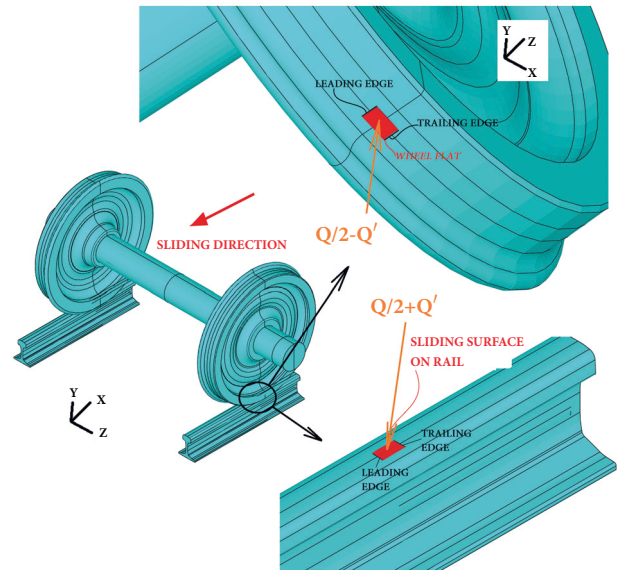

Figure 1: Pure sliding of a wheel onto rail, wheel flat on wheel tread, and sliding surface on rail. Heat generated during sliding (Q) enters equally into wheel and rail. Due to temperature difference between wheel and rail, a secondary heat (Q') transfers from wheel into rail.

Figure 1 schematically shows pure sliding of a wheel onto rail. A wheel flat is created during sliding on wheel tread and is depicted in red. The corresponding sliding surface on rail is also shown by red rectangle. Heat generated during sliding (Q) is equally divided between wheel and rail. It can be calculated as

$$Q = \mu_f mgu \tag{4}$$

where μ_f is friction coefficient of wheel and rail contact patch, m is a portion of wagon's mass which is supported by the wheel, g is gravity, and u is the sliding velocity. Due to temperature difference between wheel and rail, a secondary heat (Q') transfers from wheel into rail.

For analytical solution, semi-infinite solid assumption is made for both wheel and rail. The initial and ambient

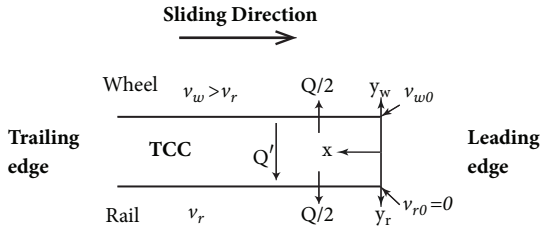

FIGURE 2: Heat transferring into sliding bodies.

temperatures are assumed to be 0°C. The real ambient temperature should be added to the results. Figure 2 shows the heat transferring into the sliding bodies.

At time zero, both bodies are at ambient temperature and $Q/2$ is transfered to each one. Later, a temperature difference will be established between them and a different heat (Q') is transferred from the warmer (wheel) into the colder (rail) body. At $(x, y_r) = (0, 0)$ the rail is always at ambient temperature because of entering a fresh rail into contact area at each moment and at this point

$$Q' = TCC.S.v_{w0}\left(y_w = 0\right) \tag{5}$$

where TCC is the thermal contact conductance and S is the contact patch area. TCC is assumed to be constant over the contact patch. During severe sliding when a wheel flat is created, this assumption is close to reality because of relatively uniform pressure distribution. At steady-state condition $Q' = Q/2$ and, from (5),

$$\frac{Q}{2} = TCC.S.v_{ws0} \tag{6}$$

where v_{ws0} indicates the steady-state value of v_{w0}. At steady-state condition, Q enters into the rail surface:

$$Q = -K_r S\frac{\partial v_r}{\partial y_r} \quad \text{at } y_r = 0. \tag{7}$$

The solution of the differential equation (2) with boundary condition of (7) gives the steady-state temperature of the rail points [10]:

$$v_{rs}\left(x, y_r\right) = \frac{2Q}{SK_r}\left[\left(\frac{\kappa_r t_r}{\pi}\right)^{1/2} e^{-y_r^2/4\kappa_r t_r} - \frac{y_r}{2} erfc\frac{y_r}{2\sqrt{\kappa_r t_r}}\right] \tag{8}$$

where t_r is sliding duration of a point on rail surface. The steady-state temperature of a rail surface point is

$$v_{rs}\left(x, y_r = 0\right) = \frac{2Q}{SK_r}\left(\frac{\kappa_r t_r}{\pi}\right)^{1/2} \tag{9}$$

and, at a constant sliding velocity (V),

$$v_{rs}\left(x, y_r = 0\right) = \frac{2Q}{SK_r}\left(\frac{\kappa_r x}{V\pi}\right)^{1/2}. \tag{10}$$

At the wheel surface,

$$\frac{Q}{2} - Q' = -K_w S\frac{dv_{w0}}{dy_w}. \tag{11}$$

From (5) and (11), it follows that

$$-\frac{dv_{w0}}{dy_w} + h_w v_{w0} = h_w v_{ws0}, \quad \left(at\ y_w = 0\right), \begin{cases} h_w = \dfrac{TCC}{K_w}, \\ v_{ws0} = \dfrac{Q}{2TCC.S} \end{cases} \tag{12}$$

v_{ws0} is constant at constant Q. The solution of differential equation (2) if $i = w0$ with boundary condition (12) is [10]

$$v_{w0} = v_{ws0}\left[erfc\frac{y_w}{2\sqrt{\kappa_w t}} - e^{h_w y_w + h_w^2\kappa_w t} erfc\left(\frac{y_w}{2\sqrt{\kappa_w t}} + h_w\sqrt{\kappa_w t}\right)\right], \quad t > 0 \tag{13}$$

The wheel surface temperature evolution at $(x, y) = (0, 0)$ can be found by inserting $y = 0$ in (13).

$$v_{w0}\left(y_w = 0\right) = v_{ws0}\left[1 - e^{h_w^2\kappa_w t} erfc\left(h_w\sqrt{\kappa_w t}\right)\right], \quad t > 0 \tag{14}$$

By inserting (14) into (5), we have

$$Q'\left(x = 0\right) = \frac{Q}{2}\left[1 - e^{h_w^2\kappa_w t} erfc\left(h_w\sqrt{\kappa_w t}\right)\right], \quad t > 0 \tag{15}$$

and the heat partitioning factor (α) can be found as

$$\alpha\left(x = 0\right) = 1 - \frac{1}{2}e^{h_w^2\kappa_w t} erfc\left(h_w\sqrt{\kappa_w t}\right), \quad t > 0. \tag{16}$$

Heat partitioning factor is defined as a portion of the frictional heat transferring into the rail during wheel skid. Then, at the rail surface,

$$f\left(t\right) = -K_r\frac{dv_r}{dy_r}, \quad \left(at\ y_r = 0\right), \quad f\left(t\right) = \frac{Q}{S}\left(1 - \frac{1}{2}e^{h_w^2\kappa_w t} erfc\left(h_w\sqrt{\kappa_w t}\right)\right) \tag{17}$$

The solution of differential equation (2) if $i = r$ assuming the rail as a semi-infinite solid with boundary condition (17) at $y_r = 0$ can be deduced from that for $f(t) = 1$ and Duhamel's principle as [10]

$$v_r = \frac{1}{K_r}\sqrt{\frac{\kappa_r}{\pi}}\int_0^{t_0}\frac{f\left(t-\tau\right)}{\sqrt{\tau}} e^{-y_r^2/4\kappa_r\tau} d\tau \tag{18}$$

where t_0 is the time duration of the heat transferring to that point of the rail during sliding and $f(t)$ is defined in (17). Equation (18) gives the rail temperature evolution. The wheel temperature on the surface can be found from (14) and (18) at $y_w = 0$ and $y_r = 0$ as

$$v_w\left(y_w = 0\right) = \frac{1}{K_r}\sqrt{\frac{\kappa_r}{\pi}}\int_0^{t_0}\frac{f\left(t-\tau\right)}{\sqrt{\tau}} d\tau + v_{ws0}\left[1 - e^{h_w^2\kappa_w t} erfc\left(h_w\sqrt{\kappa_w t}\right)\right] \tag{19}$$

t_0 depends on the velocity (V) of sliding and the position (x). Assuming a constant velocity, $t_0 = x/V$. During the

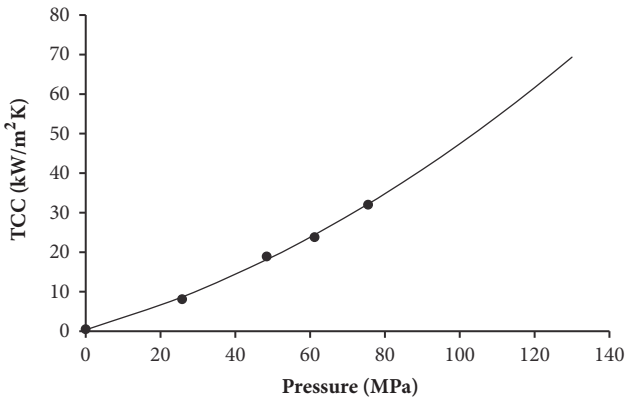

Figure 3: The variation of *TCC* with pressure [22]. A trendline is fitted to the data.

cooling period, according to Özisik [19], the distribution of temperature in wheel and rail can be calculated as

$$v_i = \frac{1}{\sqrt{4\pi\kappa_i t}} \int_{\xi=0}^{\infty} F(\xi) \left[e^{-(y_i-\xi)^2/4\kappa_i t} + e^{-(y_i+\xi)^2/4\kappa_i t} \right] d\xi, \quad (20)$$

$$i = r, w$$

$F(y_i)$ is the temperature distribution when heating ends.

Here, two real cases are considered. They are based on the report of full-scale field experiments which were performed at Silinge, Stockholm [20]. Different conditions were prepared to simulate actual situations. For example, soap water was used to reduce the friction. The average coefficients of friction in the following cases are 0.136 and 0.061, respectively. The ambient temperature for these special cases is not reported but it is generally reported as 4-17°C [21]. It is assumed as 0°C in the following cases. Otherwise, it should be added to the results.

Case 1 (freight wagon). A freight wagon with 18.9 ton axle load slides for 5.6 s with 20 km/h and an elliptical wheel flat of 25 and 11 mm radii is created and 70 kW heat is generated. We assume conductivity, mass density, and heat capacity of the wheel and rail steels as 45 W/mK, 7850 kg/m^3, and 500 J/kgK, respectively. *TCC* according to Figure 3 is 55000 W/m^{2}K [22]. The ambient temperature is assumed as 0°C.

Solution. The temperature evolution of the rail and wheel sliding surfaces along the main axis of the wheel flat can be calculated using (18) and (19) at various sliding times. Figure 4 shows temperature changing in opposite direction of sliding, along the contact area. As can be seen, the lowest temperature occurs at the leading edge of the wheel flat and the highest one at the trailing edge. At short times, the wheel temperature approaches the rail's. The rail temperature at the leading edge is always at ambient temperature (here, 0°C). The small difference between the temperature curves at 10 s sliding and 100 s sliding implies saturation or steady state of the temperature. As can be seen, the temperature changes of the wheel occur at a wider range than those of the rail. The average of the wheel surface temperature after 5.6 s sliding can be calculated [12] as 1081°C which is comparable to 1050°C that is reported by Ahlström and Karlsson [8].

In this case, the wheel temperature is sufficiently high for steel to be austenitized but the rail temperaure is lower than Ac1. During sliding, the wheel flat surface increases with time. We suppose that the wheel and rail profiles to be according to the standard UIC 920 mm freight wheel with S1002 profile and UIC60, respectively. According to the Hertzian elastic contact theory [23], the initial contact surface is an ellipse with radii 5.5 and 4.5 mm which is approximately 1/10 of the final contact surface. So, at the beginning of sliding, the heat flux is high enough to melt the wheel and rail surface layers and when the contact surface is not greater than 1/1.25 of the final wheel flat surface, the rail surface is austenitized. Because of rapid cooling into the surrounding material, creation of martensite layers is probable. Although the steady-state temperature of the rail surface is not high enough for austenitization, the rail surface is damaged at the beginning of sliding.

Figure 5 shows that the TAZ in rail is shallow during heating due to sliding. The reason is the short sliding time of each point of the rail surface. After this duration, it starts to be cooled.

The evolution of the maximum surface temperatures can be calculated from (14), (18), and (19) on the surface and is depicted in Figure 6 during 5 s sliding. According to Figure 4, the maximum surface temperature occurs at the trailing edge of the wheel flat. As can be seen, the rail temperature approaches the steady-state value faster than that of the wheel and the rate of temperature change at both wheel and rail is high at the beginning of the sliding.

Case 2 (passenger car). A passenger car with 6.2 ton axle load slides for 5 s with 39 km/h and an elliptical wheel flat of 12 mm and 6.5 mm radii is created and 20 kW heat is generated. The material property as those of Case 1 and *TCC* according to Figure 3 is 62000 W/m^{2}K [22]. We will determine the temperature evolution of the wheel and rail sliding surfaces. The ambient temperature is assumed as 0°C.

Solution. From (6), the steady-state temperature difference is calculated as 658°C. From (14), the temperature difference between wheel and rail sliding surfaces as a function of time is according to Figure 7, using the left ordinate. The change rate of temperature difference at the beginning of sliding is high and is gradually decreased to zero at steady state. This figure also shows the time evolution of heat partitioning factor using (15). It increases sharply at the beginning of sliding from 0.5 at time zero to more than 0.9 after 0.5 s. It means that, at the beginning of sliding, the frictional heat enters equally into the wheel and rail. After a short time, more than 90% of it enters into the rail. This phenomenon is called "rail chill effect" [24].

Figure 8 shows the distribution of temperature on rail sliding surface during a passage (0.0022 s) starting from (a) 0 s, (b) 0.0078 s, (c) 0.0978 s (d) 0.9978 s, and (e) 4.9978 s.

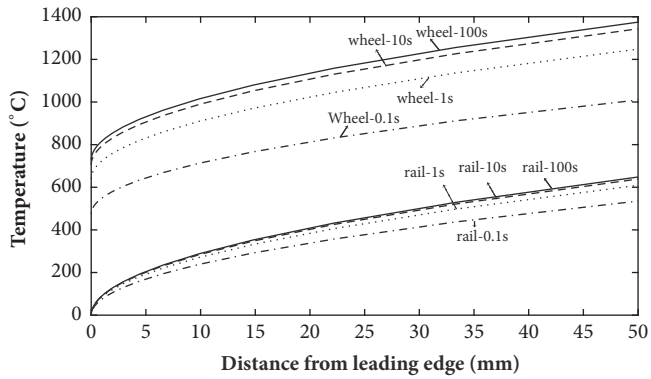

Figure 4: Distribution of surface temperature of wheel and rail after 0.1s, 1s, 10s, and 100s sliding.

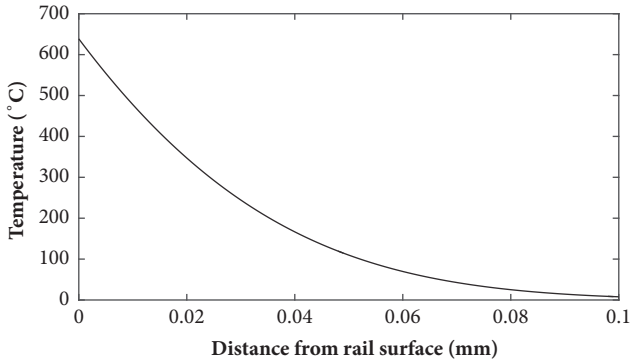

Figure 5: Distribution of the rail temperature in depth at the leading edge of the wheel flat during heating after 10 s sliding.

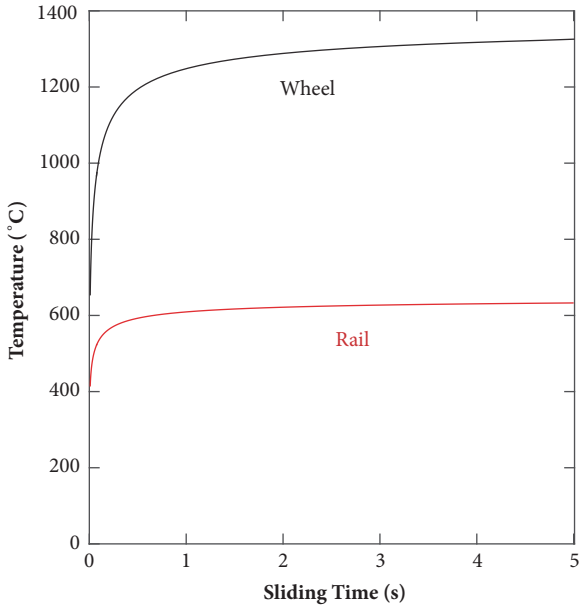

Figure 6: Time evolution of wheel and rail maximum surface temperatures during sliding.

Proximity of the lines (e.g., lines (d) and (e)) at higher times indicates reaching a steady state. At lower times, the great

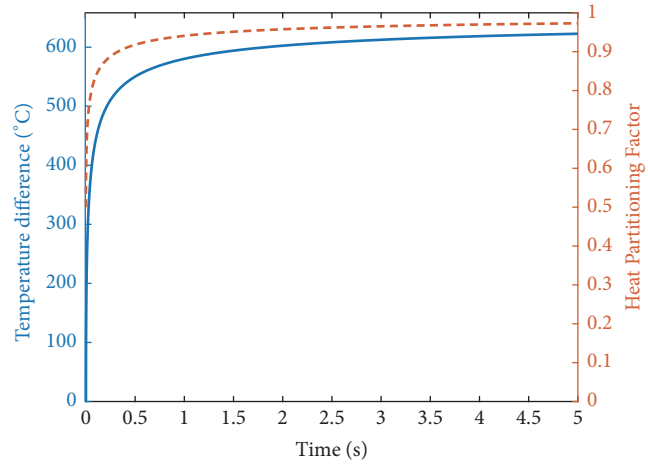

Figure 7: The temperature difference between the wheel and rail sliding surfaces (left axis), and The heat partitioning factor (right axis) vs. sliding time.

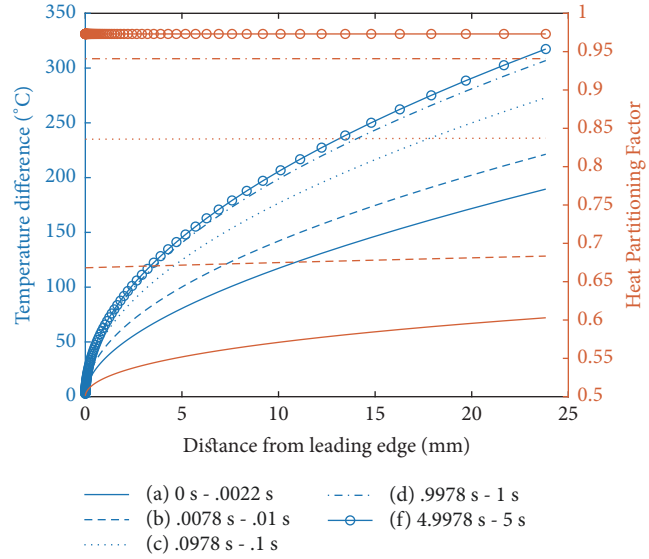

Figure 8: Distribution of temperature on rail sliding surface during a passage (0.0022s) starting from (a) 0 s, (b) 0.0078 s, (c) 0.0978 s (d) 0.9978 s, and (e) 4.9978 s.

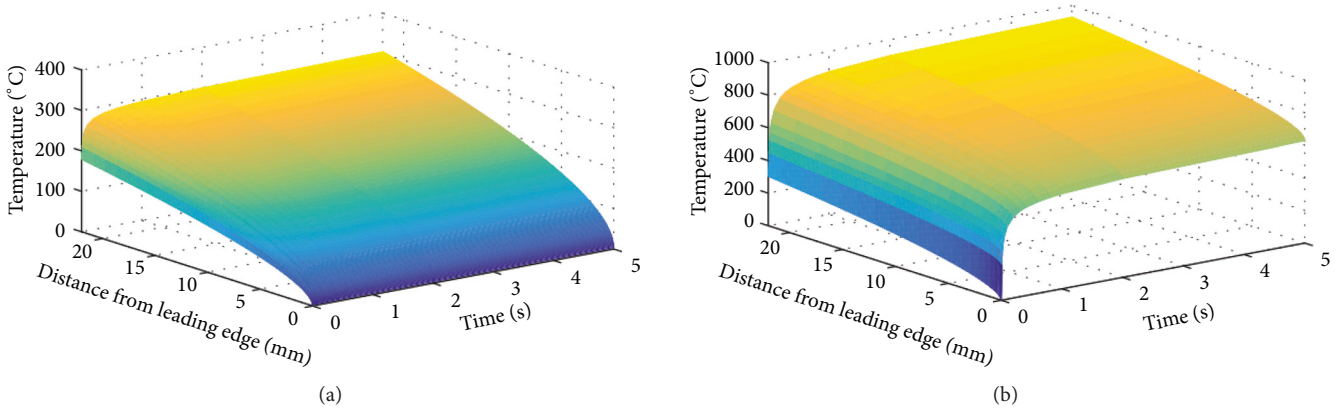

Figure 9: Temperature evolution of sliding surface of (a) rail and (b) wheel as a function of sliding time and the distance from leading edge of the wheel flat. Note that temperature limits are different in figures.

difference between them (compare lines (a), (b), and (c)) shows the rate of change. At the beginning of sliding (line (a)) during one passage, heat partitioning factor changes from 0.5 to 0.6 with a great slope. The slopes are greatly reduced at higher times.

Figure 8 can also be considered as evolution of temperature and heat partitioning factor at the trailing edge of wheel flat during a passage (0.0022 s) starting at different times (a-e). The highest temperature of this point is calculated as 316°C at 5 s. By adding the temperature difference value at 5 s from Figure 7, the maximum temperature of wheel's sliding surface at 5 s is obtained as 940°C. The average temperature at the rail surface, assuming a constant heat input into the rail during this small time interval, is obtained as 193°C [12]. The average temperature at the wheel sliding surface is calculated as 817°C, which is comparable to 800°C that is reported by Ahlström and Karlsson [8].

Figure 9 illustrates the temperature evolution of the rail and wheel sliding surfaces as a function of sliding time and the distance from the leading edge of the wheel flat. In both figures, the initial temperature at the leading edge is the ambient temperature (here, 0°C). The temperature of this point on the rail surface remains unchanged during sliding. The reason is that a fresh rail enters into contact region at this point. On the contrary, temperature of leading edge on the wheel surface increases sharply from ambient temperature (0°C) and after a short time approaches its steady-state value. This is the lowest temperature at the wheel contact surface at each moment. Temperature increases by moving away from the leading edge. The highest temperature of the wheel and rail contact surfaces occurs at the trailing edge at 5 s.

3. Conclusion

In this paper, differential equations governing the thermal analysis of the wheel and rail during sliding are solved throughout a wheel flat surface considering zero initial temperature. Because fresh rails enter into the sliding region at each moment, rail temperature at the leading edge is assumed to remain at the ambient temperature. Equations (18) and (19) give the time-history of rail and wheel surface temperature during sliding. Two real cases (a freight wagon and a passenger car) are investigated and the results are discussed. The following conclusions are obtained:

(1) During sliding, the lowest and highest temperature values occur at the leading and trailing edges of wheel flat on both wheel and rail.

(2) At the beginning of sliding during a passage, temperature and heat partitioning factor change with great slopes. These slopes are greatly reduced at higher times.

(3) The average steady-state temperature values of the wheel sliding surface in both cases considered are comparable to existing data from a field test [8] with less than 3% difference. In both cases, the calculated temperature values are higher than measured data.

(4) Using (18) and (19), temperature evolution of wheel's and rail's contact surfaces is predicted. These temperature-time histories can be used as boundary conditions on their surfaces, for example, using finite element method or any other methods, in new analyses. These can lead to find the time evolution of temperature throughout the bodies.

(5) During pure sliding of a wheel on the rail, each point at sliding region heats up as described by (18) and (19). These points cool down according to (20) when the wheel starts to roll again and the points get away from the contact region. This time-history of temperature is a prerequisite of determining the microstructural evolution at each point. Prediction of residual stress and fatigue life of a flat wheel could be the next step of this analysis.

(6) At the beginning of sliding, the heat flux may be so high because of small sliding surfaces and it can be detrimental for the wheel and rail surface layers. Creation of different defects on wheel and rail following skid can be evaluated using the results of this study.

Abbreviations

α: Heat partitioning factor
κ: Diffusivity (m^2/s) which is defined as $\kappa = K/\rho c$
λ: Rate parameter (1/s)
μ_f: Coefficient of friction
ρ: Mass density (kg/m^3)
c: Heat capacity (J/°C or J/K)
g: Gravity (m/s^2)
K: Thermal conductivity (W/m°C or W/mK)
K_0: Value of K when $v = 0$°C
m: Mass (kg)
Q: Heat generated during sliding (W)
Q': A heat which transfers from wheel into rail during sliding (W)
S: Contact patch area (m^2)
t: Time (s)
t_r: Sliding duration of a point on rail surface (s)
TCC: Thermal contact conductance (W/m^2K or $W/m^{2\circ}C$)
u: Sliding velocity (m/s)
V: A constant sliding velocity (m/s)
v: Temperature (°C)
v_{ss}: Steady-state temperature (°C)
v_{w0}: Temperature (°C) value of the wheel at $x = 0$
v_{ws0}: Steady-state value of v_{w0} (°C).

Data Availability

The output data obtained to support the findings of this study are available from the corresponding author upon request.

Conflicts of Interest

The authors declare that they have no conflicts of interest.

References

[1] A. Kapoor, "Wear by plastic ratchetting," *Wear*, vol. 212, no. 1, pp. 119–130, 1997.

[2] F. E. Kennedy, Y. Lu, and I. Baker, "Contact temperatures and their influence on wear during pin-on-disk tribotesting," *Tribology International*, vol. 82, pp. 534–542, 2015.

[3] I. Velkavrh, F. Autserer, S. Klien et al., "The influence of temperature on friction and wear of unlubricated steel/steel contacts in different gaseous atmospheres," *Tribology International*, vol. 98, pp. 155–171, 2016.

[4] A. Ekberg and E. Kabo, "Fatigue of railway wheels and rails under rolling contact and thermal loading-an overview," *Wear*, vol. 258, no. 7-8, pp. 1288–1300, 2005.

[5] K. Cvetkovski, J. Ahlström, and B. Karlsson, "Thermal softening of fine pearlitic steel and its effect on the fatigue behaviour," in *Proceedings of the 10th International Fatigue Congress, FATIGUE 2010*, pp. 541–545, Czech Republic, June 2010.

[6] C. Putignano, T. Reddyhoff, and D. Dini, "The influence of temperature on viscoelastic friction properties," *Tribology International*, vol. 100, pp. 338–343, 2016.

[7] J. Jergéus, "Martensite formation and residual stresses around railway wheel flats," *Proceedings of the Institution of Mechanical Engineers, Part C: Journal of Mechanical Engineering Science*, vol. 212, no. 1, pp. 69–79, 1998.

[8] J. Ahlström and B. Karlsson, "Analytical 1D model for analysis of the thermally affected zone formed during railway wheel skid," *Wear*, vol. 232, no. 1, pp. 15–24, 1999.

[9] H. Blok, "Les températures de surface dans des conditions de graissage sous extrême pression," in *Proceedings of the 2nd World Petroleum Congress*, 1937.

[10] H. S. Carslaw and J. C. Jaeger, *Conduction of Heat in Solids*, The Clarendon Press, Oxford, UK, 1959.

[11] J. F. Archard, "The temperature of rubbing surfaces," *Wear*, vol. 2, no. 6, pp. 438–455, 1959.

[12] J. F. Archard and R. A. Rowntree, "The temperature of rubbing bodies; part 2, the distribution of temperatures," *Wear*, vol. 128, no. 1, pp. 1–17, 1988.

[13] J. P. Srivastava, P. K. Sarkar, and V. Ranjan, "Effects of thermal load on wheel–rail contacts: A review," *Journal of Thermal Stresses*, vol. 39, no. 11, pp. 1389–1418, 2016.

[14] F. F. Ling and C. W. Ng, "On temperatures at the interfaces of bodies in sliding contact," in *Proceedings of the Fourth US Nat ional Congress of Applied Mechanics, 19G2*, 1962.

[15] J. L. González-Santander, J. M. V. Placeres, and J. M. Isidro, "Exact solution for the time-dependent temperature field in dry grinding: application to segmental wheels," *Mathematical Problems in Engineering*, vol. 2011, Article ID 927876, 28 pages, 2011.

[16] J. L. González-Santander and G. Martín, "A theorem for finding maximum temperature in wet grinding," *Mathematical Problems in Engineering*, vol. 2015, Article ID 150493, 13 pages, 2015.

[17] J. R. Barber, "Distribution of heat between sliding surfaces," *Journal of Mechanical Engineering Science*, vol. 9, no. 5, pp. 351–354, 2006.

[18] F. F. Ling and S. L. Pu, "Probable interface temperatures of solids in sliding contact," *Wear*, vol. 7, no. 1, pp. 23–34, 1964.

[19] M. N. Ozisik, *Heat Conduction*, John Willey & Sons. Inc, New York, NY, USA, 1993.

[20] J. Jergéus, C. Odenmarck, R. Lundén, P. Sotkovszki, B. Karlsson, and P. Cullers, "Full-scale railway wheel flat experiments," *Proceedings of the Institution of Mechanical Engineers, Part F: Journal of Rail and Rapid Transit*, vol. 213, no. 1, pp. 1–13, 1999.

[21] J. Jergéus, C. Odenmarck, R. Lundén, B. Karlsson, P. Sotkovszki, and P. Gullers, *The Silinge Wheel Flat Experiments*, Chalmers Solid Mechanics, Gothenburg, 20 edition, 1997.

[22] E. M. Burghold, Y. Frekers, and R. Kneer, "Determination of time-dependent thermal contact conductance through IR-thermography," *International Journal of Thermal Sciences*, vol. 98, pp. 148–155, 2015.

[23] V. L. Popov, *Contact Mechanics and Friction: Physical Principles and Applications*, Springer, Berlin, Germany, 2010.

[24] T. Vernersson and R. Lundén, "Temperatures at railway tread braking. Part 3: Wheel and block temperatures and the influence of rail chill," *Proceedings of the Institution of Mechanical Engineers, Part F: Journal of Rail and Rapid Transit*, vol. 221, no. 4, pp. 443–454, 2007.